Induced Cavities for Photonic Quantum Gates

Ohr Lahad and Ofer Firstenberg
Department of Physics of Complex Systems, Weizmann Institute of Science, Rehovot 76100, Israel
(Received 22 May 2017; published 12 September 2017)

Effective cavities can be optically induced in atomic media and employed to strengthen optical nonlinearities. Here we study the integration of induced cavities with a photonic quantum gate based on Rydberg blockade. Accounting for loss in the atomic medium, we calculate the corresponding finesse and gate infidelity. Our analysis shows that the conventional limits imposed by the blockade optical depth are mitigated by the induced cavity in long media, thus establishing the total optical depth of the medium as a complementary resource.

DOI: 10.1103/PhysRevLett.119.113601

Optical nonlinearities at the few-photon level, manifested by effective strong interactions between individual photons, provide a platform for investigating correlated photonic states [1–5] and enable optical quantum computing and networks [6–8]. The effective interaction between photons is mediated by strongly coupling them to single quantum emitters or to ensembles of cooperating emitters [9,10]. When employing single atoms, strong coupling is obtained using high-finesse optical cavities [11–15]. Cooperating ensembles, namely, interacting Rydberg atoms, can reach the strong-coupling regime without a cavity [16–20].

The cooperativity of Rydberg atoms stems from a blockade mechanism due to strong Rydberg-Rydberg interactions [21–23]. Within the so-called blockade volume, the narrow-band optical excitation of Rydberg states is limited to one collective state. Consequently, the blockade volume functions as a "superatom" with a cross section enhanced by the large number of blockaded atoms [24–26]. The optical depth $2d_B$ of the blockade volume is the key parameter determining the strength of the optical nonlinearity. For quantum nonlinear optics, high-fidelity operation of photonic gates requires $d_B \gg 1$ [5,17–19,27–31], with the fundamental limit imposed by the relation between dissipation and dispersion near resonance; see Fig. 1(a). Unfortunately, the present record $2d_B = 12.5$ [19] limits the fidelity to ~50% and is difficult to surpass [32,33].

It has been debated whether the limit imposed by d_B can be circumvented in long media, utilizing their large total optical depth $2d \gg 2d_B$; see Fig. 1(b). For example, two simultaneous photons copropagating along several blockade volumes may have longer effective interaction time, but the overall fidelity is undermined by spatial entanglement between the pulses and by the narrow transmission bandwidth in long media [5,17,27,30,34,35]. This Letter provides a positive answer to this longstanding question. We show that the Rydberg-mediated interaction can be strengthened by utilizing long media as effective cavities, whose finesse $\mathcal{F}$ grows as the square root of the total optical depth $2d$.

We employ a standing-wave dressing field to imprint a Bragg grating in the medium and induce an optical band gap. This scheme was originally proposed for enhancing nonlinear effects via dynamical control of the band gap [36,37]. We follow Hafezi *et al.* [38] and exploit the transmission resonance outside the band gap, where the Rydberg-mediated interaction is enhanced without dynamical control. The enhancement we find is similar to that obtained with actual cavities [11,39–42]: the blockaded optical depth effectively experienced by the circulating photons is given by $\mathcal{F}d_B$ [43,44]; see Fig. 1(a). To render a system with single input and output ports, as required for high-fidelity gate operation, we introduce a Sagnac configuration [Fig. 2(a)]. While the maximal finesse of optically induced cavities scales $\propto d$ [38], we show that the overall performance of a quantum phase-gate improves approximately $\propto \sqrt{d}$ when accounting for dissipation. Very recently, similar results were reported for so-called "stationary light" in the strong-coupling (noncooperative) regime [45].

Rydberg phase gate.—We analyze a gate model based on photon storage [18,35,43,44,46], illustrating the limitations posed by small d_B and the resolution offered by a cavity. Here a propagating "probe" photon acquires the

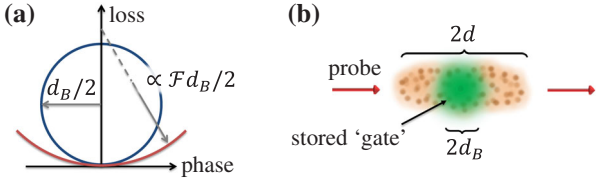

FIG. 1. (a) When light traverses an atomic medium and acquires a nonzero phase, it always experiences some loss. Given the resonant optical depth $2d_B$, the blue circle traces the relation between phase and loss for two-level atoms or under the conditions of ideal EIT [Eq. (1), see the text]. In a cavity, the radius of the circle effectively grows with the cavity finesse $\mathcal{F}$ (red). (b) A phase gate based on Rydberg blockade by a stored photon.

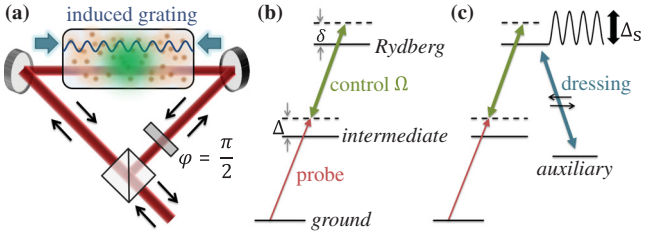

FIG. 2. (a) Optically induced grating in a Sagnac interferometer. (b) Atomic level scheme. A control field (green) couples the probe transition (red) to a Rydberg state, rendering EIT. (c) To induce a cavity, the EIT resonance frequency is longitudinally modulated by a far-detuned dressing standing wave (blue). For example, this scheme can be implemented with rubidium atoms using a probe, control, and dressing fields at 780, 479, and 475 nm, respectively. The angles between the optical axis and the dressing beams are tuned to form a standing wave with a period that is half the probe wavelength.

phase $\phi = \pi$ conditional on the storage of a "gate" photon in the medium [Fig. 1(b)]. Electromagnetically induced transparency (EIT) [47] in the ladder arrangement shown in Fig. 2(b) is employed. First, EIT is used to store the gate photon as a collective excitation comprising one Rydberg atom. Afterwards, the probe photon traverses the medium via EIT utilizing a different Rydberg level.

We use the subscripts $j = 0, 1$ to denote the cases without ($j = 0$) and with ($j = 1$) the stored Rydberg excitation. In the first case, the probe photon experiences the EIT susceptibility χ_0. In the second case, within a blockade radius r_B around the stored excitation, the EIT conditions are violated due to the Rydberg-Rydberg interaction [48], and the probe photon experiences the bare susceptibility of a two-level atom χ_1. To describe the dynamics of a single probe photon, it is sufficient to consider the linear susceptibilities of the medium. A conditional phase gate is thus obtained when $\phi = \mathrm{Re}[\chi_1 - \chi_0]kr_B = \pi$, with k being the optical wave vector.

To simplify the discussion, we include no decay of the Rydberg excitation, assuming it is negligible compared to the power broadening $|\Omega^2/(\Delta + i\Gamma)|$, with 2Ω being the Rabi frequency of the classical control field, 2Γ the decay rate of the intermediate state, and Δ the detuning from the intermediate state. The susceptibilities then acquire the form [49] $kr_B\chi_j = -d_B\Gamma/[i\Gamma + \Delta - (1-j)\Omega^2/\delta]$ for $j = 0, 1$, where d_B is the optical depth over the blockade radius r_B, and δ is the two-photon detuning from the Rydberg state. We observe that $kr_B\chi_j$ satisfy the relation [50]

$$|kr_B\chi_j - id_B/2| = d_B/2 \quad \text{for both } j = 0, 1, \tag{1}$$

forming identical circles in the complex plane; see Fig. 1(a). Therefore, loss of the probe photon ($\propto \mathrm{Im}\chi_j$) is unavoidable whenever $\phi \neq 0$, which limits the gate fidelity. The operating point that minimizes the loss has an elegant solution when the whole medium is blocked ($d = d_B$ [19]). Then, the loss is quantified by the mean absorption with and without the stored Rydberg excitation $\epsilon = \mathrm{Im}[\chi_1 + \chi_0]kr_B$, and we observe that ϕ and ϵ form a circle too, now with twice the radius $|\phi + i\epsilon - id_B| = d_B$. It follows that $\phi = \pi$ requires $d_B \geq \pi$; for $d_B \gg \pi$, the loss $\epsilon = \pi^2/(2d_B)$ scales inversely with d_B.

The above limitation can be overcome by incorporating an optical cavity with single input and output ports, such as single-side cavities [12–14,43,44,51] or ring cavities [15,52,53]. For example, consider a ring cavity of length l containing the atomic medium [Fig. 3(a)]. With ρ being the reflection amplitude of the coupling mirror, the cavity output amplitude is given by $u_j = (\rho + e^{i\theta_j})/(1 + \rho e^{i\theta_j})$ [54]. The (complex) phase acquired along the ring $\theta_j = kl + kr_B\chi_j$ includes the medium response with ($j = 1$) and without ($j = 0$) the stored Rydberg excitation. For a bare cavity tuned to resonance $kl = \pi$, gating the medium between χ_0 and χ_1 shifts the cavity across its resonance and alters the reflected phase from $-\pi/2$ to $\pi/2$. Minimal absorption from the medium is obtained around the bottom of the circles described by Eq. (1), where $\mathrm{Im}[kr_B\chi_j] \approx \mathrm{Re}[kr_B\chi_j]^2/d_B$. Substituting this into θ_j and u_j, and defining again the loss and conditional phase

$$\begin{aligned} \epsilon &= -\log(|u_1|) - \log(|u_0|), \\ \phi &= \arg(u_1) - \arg(u_0), \end{aligned} \tag{2}$$

we find the relation

$$\epsilon = (4\pi)/(\mathcal{F}d_B)[1 - \cos(\phi/2)], \tag{3}$$

where the finesse $\mathcal{F} = \pi(1+\rho)/(1-\rho)$. For $\phi = \pi$ and comparing to $\epsilon = \pi^2/(2d_B)$ obtained without a cavity, we find that d_B is effectively increased by the factor $\pi\mathcal{F}/8$; see Fig. 3(b).

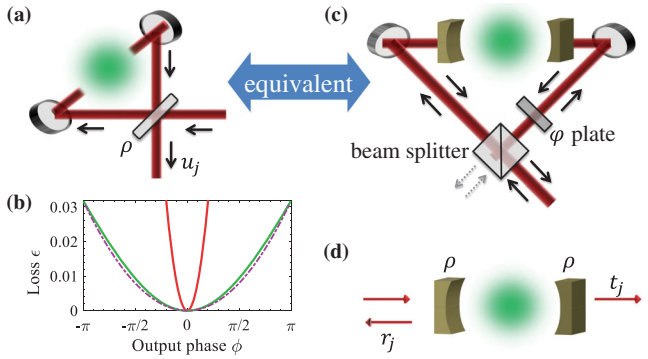

FIG. 3. Cavities encircling atomic media. (a) Ring cavity. (b) The loss vs phase, defined in Eq. (2), for the ring cavity ($\mathcal{F} = 20\pi$, $2d_B = 4\pi$). The exact relation in Eq. (3) (green) is well approximated by a circle (dashed purple) with a radius $\pi\mathcal{F}/8$ larger than that obtained with no cavity (red). (c) A symmetric Fabry-Pérot cavity inside a Sagnac interferometer is equivalent to a ring cavity. (d) Fabry-Pérot cavity.

A cavity induced by uniformly dressing the medium, as we shall analyze, is akin to a symmetric Fabry-Pérot cavity, with two pairs of input-output ports. To recover a single-port configuration, we place the two-port cavity inside a Sagnac interferometer, as depicted in Fig. 3(c). The incoming light impinges on the cavity from both sides, with the relative phase tuned by a phase plate φ.

The transmission matrix from the external input ports to the external output ports of the Sagnac beam splitter (BS) is calculated from

$$\overbrace{\frac{1}{2}\begin{pmatrix}1 & i\\ i & 1\end{pmatrix}}^{\text{BS out}}\overbrace{\begin{pmatrix}1 & 0\\ 0 & e^{i\varphi}\end{pmatrix}}^{\varphi\text{-plate}}\overbrace{\begin{pmatrix}0 & 1\\ 1 & 0\end{pmatrix}}^{\text{flip modes}}\overbrace{\begin{pmatrix}t_j & r_j\\ r_j & t_j\end{pmatrix}}^{\text{cavity}}\overbrace{\begin{pmatrix}1 & 0\\ 0 & e^{i\varphi}\end{pmatrix}}^{\varphi\text{-plate}}\overbrace{\begin{pmatrix}1 & i\\ i & 1\end{pmatrix}}^{\text{BS in}}, \tag{4}$$

with the transmission and reflection amplitudes of the bare cavity [see Fig. 3(d)] given by [55]

$$t_j = \frac{(1-\rho^2)e^{i\theta_j}}{1+\rho^2 e^{2i\theta_j}} \quad \text{and} \quad r_j = i\frac{\rho(1+e^{2i\theta_j})}{1+\rho^2 e^{2i\theta_j}}. \tag{5}$$

By choosing $\varphi = \pi/2$, the matrix (4) becomes diagonal, and the light is back reflected to the port it arrived from. The output amplitude for the first port is $r_j - t_j$, which exactly equals iu_j of the ring cavity (with the shift $\theta_j \mapsto \theta_j - \pi/2$). Therefore, while the phase shift of a bare two-port cavity is limited to $\pi/2$ per port around the resonance [56], the Sagnac setup enables a π conditional phase shift, regaining the single-port properties. We stress that the Sagnac interferometer does not form another cavity, and field buildup occurs only inside the cavity.

Bragg grating.—We now turn to consider cavities formed by finite media with a uniform longitudinal modulation. A modulation on the wavelength scale couples the right (+) and left (−) propagating modes $E_\pm(z)$ according to

$$\frac{\partial \vec{E}(z)}{\partial z} = i\begin{pmatrix}\sigma & \kappa\\ -\kappa & -\sigma\end{pmatrix}\vec{E}(z), \quad \text{where } \vec{E}(z) = \begin{pmatrix}E_+(z)\\ E_-(z)\end{pmatrix}. \tag{6}$$

For example, in a Bragg grating with a modulated susceptibility $\chi(z) = \chi_{\rm DC} + \chi_{\rm AC}\cos(2k_s z)$, the coupling matrix elements for a probe with wave number k are given by $\sigma = k - k_s + k\chi_{\rm DC}/2$ and $\kappa = k\chi_{\rm AC}/4$ [57]. The solution of Eq. (6) can be written for a uniform grating of length L as $\vec{E}(z) = \mathbf{F}_{L-z}\vec{E}(L)$, where

$$\mathbf{F}_z = \frac{1}{\lambda}\begin{pmatrix}\lambda\cos(\lambda z) - i\sigma\sin(\lambda z) & -i\kappa\sin(\lambda z)\\ i\kappa\sin(\lambda z) & \lambda\cos(\lambda z) + i\sigma\sin(\lambda z)\end{pmatrix},$$

with the eigenvalues $\pm\lambda = \pm\sqrt{\sigma^2-\kappa^2}$. For a field incoming at $z = 0$, we substitute $E_+(L) = 1$ and $E_-(L) = 0$ and obtain the transmission and reflection coefficients, $t_0 = 1/E_+(0)$ and $r_0 = E_-(0)/E_+(0)$. The transmission spectrum, shown in Fig. 4(a) for a specific set of parameters, exhibits a wide reflection "band gap" at $\sigma \approx 0$ and narrow transmission resonances around it. These resonances arise due to the finite length of the medium and correspond to the oscillations of $\mathbf{F}_z$ outside the band gap, where the eigenvalues $\pm\lambda$ are predominantly real. The intensity profiles along the medium $\|\vec{E}(z)\|^2 = |E_+^2| + |E_-^2|$ at the first four resonances $\mathrm{Re}(\lambda L) \approx m\pi$ $(m = 1\text{–}4)$ are shown in the inset of Fig. 4(a). The intensity builds up in the bulk, similarly to a cavity resonance [38,57].

The limitation discussed earlier for Fabry-Pérot cavities applies here as well—the symmetric two-port cavity formed by the uniform grating cannot alone perform an efficient conditional π-phase operation. We thus invoke the Sagnac setup, as depicted in Fig. 2(a). Then the overall output amplitude calculated from (4) is $r_0 - t_0$, and the field in the bulk is

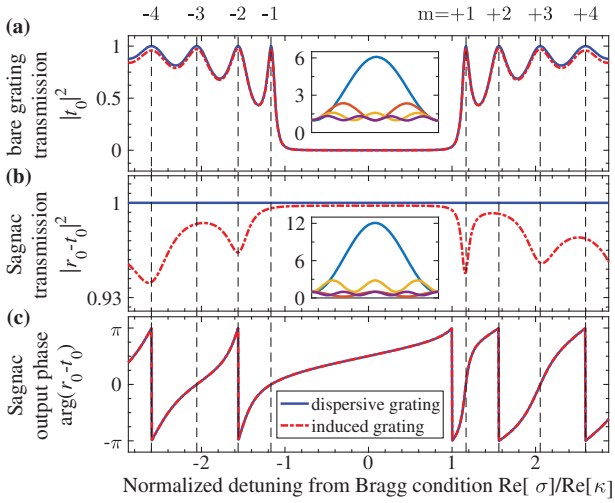

FIG. 4. Transmission spectra of (a) bare Bragg grating, and [(b) and (c)] grating inside a Sagnac interferometer. We compare (solid blue) a purely dispersive Bragg grating ($\kappa L = 5.24$, $\mathrm{Im}\sigma = 0$) with (dashed red) a grating formed by dressing an atomic medium ($d = 10^4$, and the dressing parameters are chosen to minimize the gate loss when $2d_B = 4\pi$). The resonances of the bare grating are $m = \pm(1, 2, 3, 4, \ldots)$, but only $m = 1, -2, 3, -4, \ldots$ retain the steep phase slope in the Sagnac setup. Insets: longitudinal intensity profiles $\|\vec{E}(z)\|^2$ at the corresponding resonances $\pm m = 1\text{–}4$ (blue, red, orange, and purple).

$$\vec{E}_{\mathrm{Sag}}(z)=\frac{1}{\sqrt{2}}\left[\vec{E}(z)-\begin{pmatrix}0&1\\1&0\end{pmatrix}\vec{E}(L-z)\right]. \quad (7)$$

Figures 4(b) and 4(c) show the resulting spectrum and the intensity profiles at the first four resonances. Evidently, only the resonances $m=+1,-2,+3,-4,\ldots$, having antisymmetric modes, are enhanced in the Sagnac setup. At these resonances, the slope of the output phase and the intensity buildup $B=\max_z\|\vec{E}_{\mathrm{Sag}}(z)\|^2>1$ scale linearly with the effective finesse $\mathcal{F}\approx\pi B$. The strongest resonance is obtained for $m=+1$, where $\lambda L=\pi(1+i\alpha)$. Up to first order in the loss $\alpha\ll 1$, we find the overall transmissivity T and finesse $\mathcal{F}$,

$$T=|r_0-t_0|^2\approx\left|\frac{1-\alpha\kappa L}{1+\alpha\kappa L q}\right|^2 \quad \text{and}$$
$$\mathcal{F}\approx\frac{1}{\pi}\left|\frac{(1+q)\kappa L}{1+\alpha\kappa L q}\right|^2, \quad (8)$$

where $q=\sqrt{1+\pi^2/(\kappa L)^2}$.

Induced cavities in atomic media.—The atomic scheme we analyze in order to optically induce a grating is shown in Fig. 2(c). A standard Rydberg EIT system as outlined earlier is coupled to an auxiliary atomic state by a dressing standing wave with wave vector $k_s\approx k$ [36]. The far-detuned dressing field gives rise to a longitudinally periodic light shift of the Rydberg state, effectively modulating the two-photon detuning $\delta_{\mathrm{mod}}(z)=\delta+\Delta_s\cos(2k_sz)$. Staying well within the EIT linewidth $|\delta_{\mathrm{mod}}|\ll|\Omega^2/(\Delta+i\Gamma)|$, the EIT susceptibility $kL\chi_0=-2d\Gamma/(i\Gamma+\Delta-\Omega^2/\delta_{\mathrm{mod}})$ can be expanded as

$$\chi_0(z)\approx\frac{2d}{kL}\frac{\delta_{\mathrm{mod}}(z)}{\Omega^2/\Gamma}\left(1+i\frac{\delta_{\mathrm{mod}}(z)}{\Omega^2/(\Gamma-i\Delta)}\right). \quad (9)$$

We now substitute $2\cos^2(2k_sz)=1+\cos(4k_sz)$ and neglect the fast oscillating term $\cos(4k_sz)$ [36,58]. The terms proportional to $\cos(2k_sz)$ are identified as χ_{AC}, and the rest comprise χ_{DC}. Finally, the Bragg coupling coefficients are given by [57]

$$\sigma=\Delta k+k\frac{\chi_{\mathrm{DC}}}{2}=\Delta k+\frac{d}{L}\left[x+(x^2+2y^2)\left(i+\frac{\Delta}{\Gamma}\right)\right]$$
$$\kappa=k\frac{\chi_{\mathrm{AC}}}{4}=\frac{d}{L}\left[y+2xy\left(i+\frac{\Delta}{\Gamma}\right)\right], \quad (10)$$

where $x=\delta\Gamma/\Omega^2$, $y=\Delta_s\Gamma/(2\Omega^2)$, and $\Delta k=k-k_s$. The imaginary parts of σ and κ account for loss, absent in an ideal Bragg grating.

We focus on the first resonance $\lambda L=\pi(1+i\alpha)$. Assuming a frequency modulation well within the EIT line $x,y\ll 1$, the absorption is given by $\alpha=d^2x^3/\pi^2$. With this and Eq. (9), in the large d limit, the finesse is insensitive to Δ/Γ and becomes $\mathcal{F}=(1+\sqrt{T})\sqrt{(1-T)d}$ (see Ref. [59] for details). The maximal finesse $\mathcal{F}\approx 1.3\sqrt{d}$ is obtained for $T=1/4$, as shown in Fig. 5.

The loss $T<1$ is of course the unavoidable downside of using atomic resonances, and we desire to maximize T and $\mathcal{F}$ simultaneously. For $1-T\ll 1$, the tradeoff arising from $\mathcal{F}\propto\sqrt{1-T}$ can be heuristically estimated by adding $1-T$ to the loss ϵ in Eq. (3) and minimizing ϵ with respect to $\mathcal{F}$. The result is $\mathcal{F}\approx\sqrt[3]{8\pi d/d_B}$, which scales as $\sqrt[3]{d}$ rather than $\sqrt{d}$ [59].

We find by numerical optimization that the exact performance of the scheme is slightly better than the above estimation. In the numerics, we describe the blockade effect around the stored Rydberg excitation using the susceptibility χ_1 at $|z-L/2|<r_B$. Outside the blockade volume, we use Eq. (6), so that the medium transmission is described by

$$\vec{E}(0)=\mathbf{F}_{\frac{L}{2}-r_B}\begin{pmatrix}e^{-ikr_B\chi_1}&0\\0&e^{ikr_B\chi_1}\end{pmatrix}\mathbf{F}_{\frac{L}{2}-r_B}\vec{E}(L). \quad (11)$$

We calculate the Sagnac output $iu_j=r_j-t_j$, substitute into Eq. (2), and minimize the loss ϵ while requiring $\phi=\pi$. As shown in Fig. 5, the optimization finds that ϵ scales as $\sim d^{-0.43}$. We conclude that optically induced cavities can enhance the performance of photonic quantum gates.

We have examined a specific extension of EIT, utilizing far-detuned dressing. An alternative extension is a dual-V configuration rendering stationary light [37,45,58,60,61]. Here counterpropagating control fields couple the two propagation directions of the probe fields via resonant four-wave mixing. We have repeated our analysis for this scheme. As shown by Hafezi *et al.* [38], this scheme affords a higher maximal finesse $\mathcal{F}\propto d$, but our optimization yields an overall scaling of $1/\epsilon$ slower than $\sqrt{d}$ when accounting for the reduced transmission $T<1$, as also reported in Ref. [45].

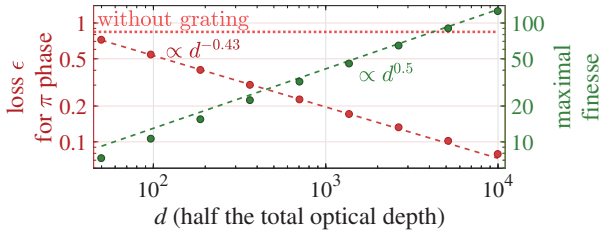

FIG. 5. Scaling of performance with optical depth. Green: numerical maximization of the induced cavity finesse (dots) compared to the analytic result $\mathcal{F}\approx 1.3\sqrt{d}$ (line). Red: numerical minimization of the loss for a phase gate with $2d_B=4\pi$ (dots) and a power-law fit (line). For example, for $d=10^4$, the optimization finds $\epsilon=0.08$ at $x=6.0\times10^{-4}$, $y=5.2\times10^{-4}$. The dashed lines in Figs. 4(b) and 4(c) are plotted for $y=5.2\times10^{-4}$ and scanning x. Without the induced grating, the loss is very high ($\epsilon\approx 1$; horizontal orange line). See Ref. [59] for more details on the optimized parameters.

Conclusions.—We showed that optical modulation of a finite medium can form an effective cavity that strengthens photon-photon interactions based on Rydberg blockade. The inadequacy of a symmetric (two-port) cavity for a conditional π-phase operation is solved with a Sagnac interferometer. We benchmark the induced cavity by calculating the phase-loss relation in a Rydberg-based phase gate. This relation is described approximately by a circle, whose radius scales linearly with $d_B\mathcal{F}$. For the specific atomic system we consider, the finesse of the induced cavity scales roughly as $\mathcal{F} \propto d^{0.4}$ (when optimized together with the overall transmission), and thus so is the effective enhancement of d_B. By this we establish that the optical depth of the medium outside the blockade volume is a complementary resource to the limited d_B. The essential ingredient of the scheme is the coupling between the counterpropagating modes. This coupling delays an incoming probe pulse via so-called "structural" slow light, as opposed to the standard delay due to EIT, pertaining to "material" slow light [62]. While the latter maintains the amplitude of the incoming probe field, the former increases it in the medium.

Optically induced band gaps were demonstrated experimentally using several atomic level schemes [60,63,64]. The proposed induced cavities are realizable with the optical depths of $10^3 - 10^5$ obtained with either cold [65,66] or hot [67] atoms. As a general concept, induced cavities could be employed in other systems, where actual cavities are impractical or for switchable functionality of photonic devices.

We thank A. Gorshkov, B. Dayan, and S. Hofferberth for fruitful discussions, and C. Avinadav for helpful comments on the manuscript. We acknowledge financial support by the Israel Science Foundation and ICORE, the European Research Council starting investigator Grant No. Q-PHOTONICS 678674, the Minerva Foundation, the Sir Charles Clore research prize, and the Laboratory in Memory of Leon and Blacky Broder.

[1] I. Carusotto and C. Ciuti, Quantum fluids of light, Rev. Mod. Phys. **85**, 299 (2013).
[2] J. Otterbach, M. Moos, D. Muth, and M. Fleischhauer, Wigner Crystallization of single photons in cold Rydberg ensembles, Phys. Rev. Lett. **111**, 113001 (2013).
[3] E. Shahmoon, P. Grišins, H. P. Stimming, I. Mazets, and G. Kurizki, Highly nonlocal optical nonlinearities in atoms trapped near a waveguide, Optica **3**, 725 (2016).
[4] M. F. Maghrebi, M. J. Gullans, P. Bienias, S. Choi, I. Martin, O. Firstenberg, M. D. Lukin, H. P. Büchler, and A. V. Gorshkov, Coulomb Bound States of Strongly Interacting Photons, Phys. Rev. Lett. **115**, 123601 (2015).
[5] O. Firstenberg, T. Peyronel, Q.-Y. Liang, A. V. Gorshkov, M. D. Lukin, and V. Vuletić, Attractive photons in a quantum nonlinear medium, Nature (London) **502**, 71 (2013).
[6] J. L. O'Brien, Optical Quantum Computing, Science **318**, 1567 (2007).
[7] J. L. O'Brien, A. Furusawa, and J. Vučković, Photonic quantum technologies, Nat. Photonics **3**, 687 (2009).
[8] H. J. Kimble, The Quantum Internet, Nature (London) **453**, 1023 (2008).
[9] D. E. Chang, V. Vuletić, and M. D. Lukin, Quantum nonlinear optics photon by photon, Nat. Photonics **8**, 685 (2014).
[10] D. Roy, C. M. Wilson, and O. Firstenberg, Colloquium: Strongly interacting photons in one-dimensional continuum, Rev. Mod. Phys. **89**, 021001 (2017).
[11] H. Tanji-Suzuki, I. D. Leroux, M. H. Schleier-Smith, M. Cetina, A. T. Grier, J. Simon, and V. Vuletić, Interaction between Atomic Ensembles and Optical Resonators: Classical Description, Adv. At. Mol. Opt. Phys. **60**, 201 (2011).
[12] L. M. Duan and H. J. Kimble, Scalable photonic quantum computation through cavity-assisted interactions, Phys. Rev. Lett. **92**, 127902 (2004).
[13] B. Hacker, S. Welte, G. Rempe, and S. Ritter, A photon-photon quantum gate based on a single atom in an optical resonator, Nature (London) **536**, 193 (2016).
[14] T. G. Tiecke, J. D. Thompson, N. P. de Leon, L. R. Liu, V. Vuletić, and M. D. Lukin, Nanophotonic quantum phase switch with a single atom, Nature (London) **508**, 241 (2014).
[15] J. Volz, M. Scheucher, C. Junge, and A. Rauschenbeutel, Nonlinearπ phase shift for single fibre-guided photons interacting with a single resonator-enhanced atom, Nat. Photonics **8**, 965 (2014).
[16] O. Firstenberg, C. S. Adams, and S. Hofferberth, Nonlinear quantum optics mediated by Rydberg interactions, J. Phys. B **49**, 152003 (2016).
[17] T. Peyronel, O. Firstenberg, Q.-Y. Liang, S. Hofferberth, A. V. Gorshkov, T. Pohl, M. D. Lukin, and V. Vuletić, Quantum nonlinear optics with single photons enabled by strongly interacting atoms, Nature (London) **488**, 57 (2012).
[18] D. Tiarks, S. Schmidt, G. Rempe, and S. Du rr, Optical phase shift created with a single-photon pulse, Sci. Adv. **2**, e1600036 (2016).
[19] C. Tresp, C. Zimmer, I. Mirgorodskiy, H. Gorniaczyk, A. Paris-Mandoki, and S. Hofferberth, Single-Photon Absorber Based on Strongly Interacting Rydberg Atoms, Phys. Rev. Lett. **117**, 223001 (2016).
[20] J. D. Pritchard, K. J. Weatherill, and C. S. Adams, Nonlinear optics using cold Rydberg atoms, Annu. Rev. Cold At. Mol. **1**, 301 (2013).
[21] M. D. Lukin, M. Fleischhauer, R. Cote, L. M. Duan, D. Jaksch, J. I. Cirac, and P. Zoller, Dipole Blockade and Quantum Information Processing in Mesoscopic Atomic Ensembles, Phys. Rev. Lett. **87**, 037901 (2001).
[22] M. Saffman, T. G. Walker, and K. Mølmer, Quantum information with Rydberg atoms, Rev. Mod. Phys. **82**, 2313 (2010).
[23] J. D. Pritchard, D. Maxwell, A. Gauguet, K. J. Weatherill, M. P. A. Jones, and C. S. Adams, Cooperative atom-light interaction in a blockaded Rydberg ensemble, Phys. Rev. Lett. **105**, 193603 (2010).
[24] V. Vuletic, Quantum networks: When superatoms talk photons, Nat. Phys. **2**, 801 (2006).
[25] T. A. Johnson, E. Urban, T. Henage, L. Isenhower, D. D. Yavuz, T. G. Walker, and M. Saffman, Rabi oscillations

between ground and Rydberg States with dipole-dipole atomic interactions, Phys. Rev. Lett. **100**, 113003 (2008).
[26] Y. O. Dudin, L. Li, F. Bariani, and A. Kuzmich, Observation of coherent many-body Rabi oscillations, Nat. Phys. **8**, 790 (2012).
[27] A. V. Gorshkov, R. Nath, and T. Pohl, Dissipative many-body quantum optics in Rydberg media, Phys. Rev. Lett. **110**, 153601 (2013).
[28] D. Paredes-Barato and C. S. Adams, All-optical quantum information processing using Rydberg gates, Phys. Rev. Lett. **112**, 040501 (2014).
[29] M. Moos, M. Höning, R. Unanyan, and M. Fleischhauer, Many-body physics of Rydberg dark-state polaritons in the strongly interacting regime, Phys. Rev. A **92**, 053846 (2015).
[30] C. R. Murray, A. V. Gorshkov, and T. Pohl, Many-body decoherence dynamics and optimized operation of a single-photon switch, New J. Phys. **18**, 092001 (2016).
[31] C. R. Murray and T. Pohl, Coherent Photon Manipulation in Interacting Atomic Ensembles, Phys. Rev. X **7**, 031007 (2017).
[32] A. Gaj, A. T. Krupp, J. B. Balewski, R. Löw, S. Hofferberth, and T. Pfau, From molecular spectra to a density shift in dense Rydberg gases, Nat. Commun. **5**, 4546 (2014).
[33] S. Baur, D. Tiarks, G. Rempe, and S. Dürr, Single-Photon Switch Based on Rydberg Blockade, Phys. Rev. Lett. **112**, 073901 (2014).
[34] P. Bienias and H. P. Büchler, Quantum theory of Kerr nonlinearity with Rydberg slow light polaritons, New J. Phys. **18**, 123026 (2016).
[35] W. Li and I. Lesanovsky, Coherence in a cold-atom photon switch, Phys. Rev. A **92**, 043828 (2015).
[36] A. André and M. D. Lukin, Manipulating Light Pulses via Dynamically Controlled Photonic Band gap, Phys. Rev. Lett. **89**, 143602 (2002).
[37] A. André, M. Bajcsy, A. S. Zibrov, and M. D. Lukin, Nonlinear Optics with Stationary Pulses of Light, Phys. Rev. Lett. **94**, 063902 (2005).
[38] M. Hafezi, D. E. Chang, V. Gritsev, E. Demler, and M. D. Lukin, Quantum transport of strongly interacting photons in a one-dimensional nonlinear waveguide, Phys. Rev. A **85**, 013822 (2012).
[39] V. Parigi, E. Bimbard, J. Stanojevic, A. J. Hilliard, F. Nogrette, R. Tualle-Brouri, A. Ourjoumtsev, and P. Grangier, Observation and Measurement of Interaction-Induced Dispersive Optical Nonlinearities in an Ensemble of Cold Rydberg Atoms, Phys. Rev. Lett. **109**, 233602 (2012).
[40] J. Ningyuan, A. Georgakopoulos, A. Ryou, N. Schine, A. Sommer, and J. Simon, Observation and characterization of cavity Rydberg polaritons, Phys. Rev. A **93**, 041802 (2016).
[41] J.-F. Roch, K. Vigneron, P. Grelu, A. Sinatra, J.-P. Poizat, and P. Grangier, Quantum Nondemolition Measurements using Cold Trapped Atoms, Phys. Rev. Lett. **78**, 634 (1997).
[42] A. V. Gorshkov, A. André, M. D. Lukin, and A. S. Sørensen, Photon storage in Λ-type optically dense atomic media. III. Effects of inhomogeneous broadening, Phys. Rev. A **76**, 033806 (2007).
[43] S. Das, A. Grankin, I. Iakoupov, E. Brion, J. Borregaard, R. Boddeda, I. Usmani, A. Ourjoumtsev, P. Grangier, and A. S. Sørensen, Photonic controlled- phase gates through Rydberg blockade in optical cavities, Phys. Rev. A **93**, 040303 (2016).
[44] Y. M. Hao, G. W. Lin, K. Xia, X. M. Lin, Y. P. Niu, and S. Q. Gong, Quantum controlled-phase-flip gate between a flying optical photon and a Rydberg atomic ensemble, Sci. Rep. **5**, 10005 (2015).
[45] I. Iakoupov, J. Borregaard, and A. S. Srensen, Controlled-phase gate for photons based on stationary light, arXiv:1610.09206.
[46] A. V. Gorshkov, J. Otterbach, M. Fleischhauer, T. Pohl, and M. D. Lukin, Photon-photon interactions via Rydberg blockade, Phys. Rev. Lett. **107**, 133602 (2011).
[47] M. Fleischhauer, A. Imamoglu, and J. P. Marangos, Electromagnetically induced transparency: Optics in coherent media, Rev. Mod. Phys. **77**, 633 (2005).
[48] A. Reinhard, T. C. Liebisch, B. Knuffman, and G. Raithel, Level shifts of rubidium Rydberg states due to binary interactions, Phys. Rev. A **75**, 032712 (2007).
[49] E. Paspalakis and P. L. Knight, Electromagnetically induced transparency and controlled group velocity in a multilevel system, Phys. Rev. A **66**, 015802 (2002).
[50] In fact, all multilevel EIT susceptibilities $\chi = \chi_1[1-\sum_n \Omega_n^2/(\delta_n + i\gamma_n)/(\Delta + i\Gamma)]^{-1}$ with multiple Rabi frequencies Ω_n and detunings δ_n [49] form the same circle when $\gamma_n = 0$.
[51] E. Waks and J. Vuckovic, Dispersive properties and large Kerr nonlinearities using dipole-induced transparency in a single-sided cavity, Phys. Rev. A **73**, 041803(R) (2006).
[52] I. Shomroni, S. Rosenblum, Y. Lovsky, O. Bechler, G. Guendelman, and B. Dayan, All-optical routing of single photons by a one-atom switch controlled by a single photon, Science **345**, 903 (2014).
[53] R. Ritter, N. Gruhler, W. H. P. Pernice, H. Kübler, T. Pfau, and R. Löw, Coupling thermal atomic vapor to an integrated ring resonator, New J. Phys. **18**, 103031 (2016).
[54] A. Yariv and P. Yeh, *Photonics: Optical Electronics in Modern Communications* (Oxford University Press, New York, 2006).
[55] A. E. Siegman, *Lasers* (University Science Books, Sausalito, CA, 1986).
[56] For example, $|\arg(r_0)-\arg(r_1)|<\pi/2$ and $|\arg(t_0)-\arg(t_1)|<\pi/2$ within the resonance linewidth $|\mathrm{Re}(\theta_0-\theta_1)|<\pi/\mathcal{F}$.
[57] T. Erdogan, Fiber grating spectra, J. Lightwave Technol. **15**, 1277 (1997).
[58] F. E. Zimmer, A. André, M. D. Lukin, and M. Fleischhauer, Coherent control of stationary light pulses, Opt. Commun. **264**, 441 (2006).
[59] See Supplemental Material at http://link.aps.org/supplemental/10.1103/PhysRevLett.119.113601 for more details on the optimization of parameters.
[60] M. Bajcsy, A. S. Zibrov, and M. D. Lukin, Stationary pulses of light in an atomic medium, Nature (London) **426**, 638 (2003).
[61] I. Iakoupov, J. R. Ott, D. E. Chang, and A. S. Sørensen, Dispersion relations for stationary light in one-dimensional atomic ensembles, Phys. Rev. A **94**, 053824 (2016).
[62] R. W. Boyd, Material slow light and structural slow light: similarities and differences for nonlinear optics, J. Opt. Soc. Am. B **29**, 2644 (2012).

[63] B. Little, D. J. Starling, J. C. Howell, R. D. Cohen, D. Shwa, and N. Katz, Rapidly reconfigurable optically induced photonic crystals in hot rubidium vapor, Phys. Rev. A **87**, 043815 (2013).

[64] Y. W. Lin, W. T. Liao, T. Peters, H. C. Chou, J. S. Wang, H. W. Cho, P. C. Kuan, and I. A. Yu, Stationary light pulses in cold atomic media and without Bragg gratings, Phys. Rev. Lett. **102**, 213601 (2009).

[65] B. M. Sparkes, J. Bernu, M. Hosseini, J. Geng, Q. Glorieux, P. A. Altin, P. K. Lam, N. P. Robins, and B. C. Buchler, Gradient echo memory in an ultra-high optical depth cold atomic ensemble, New J. Phys. **15**, 085027 (2013).

[66] F. Blatt, T. Halfmann, and T. Peters, One-dimensional ultracold medium of extreme optical depth, Opt. Lett. **39**, 446 (2014).

[67] K. T. Kaczmarek, D. J. Saunders, M. R. Sprague, W. S. Kolthammer, A. Feizpour, P. M. Ledingham, B. Brecht, E. Poem, I. A. Walmsley, and J. Nunn, Ultrahigh and persistent optical depths of cesium in Kagomé-type hollow-core photonic crystal fibers, Opt. Lett. **40**, 5582 (2015).